Fundamenta Informaticae 75 (2007) 483–504

Histogram Thresholding using Beam Theory and Ambiguity Measures*

Debashis Sen† and Sankar K. Pal

Center for Soft Computing Research

Indian Statistical Institute

203 B.T. Road, Kolkata, West Bengal, India 700108

{*dsen_t, sankar*}*@isical.ac.in*

Abstract. This paper presents a novel histogram thresholding technique based on the beam theory of solid mechanics and the minimization of ambiguity in information. First, a beam theory based histogram modification process is carried out. This beam theory based process considers a distance measure in order to modify the shape of the histogram. The ambiguity in the overall information given by the modified histogram is then minimized to obtain the threshold value. The ambiguity minimization is carried out using the theories of fuzzy and rough sets, where a new definition of rough entropy is presented. The applications of the proposed scheme in performing object and edge extraction in images are reported and compared with those of a few existing classical and ambiguity minimization based schemes for thresholding. Experimental results are given to demonstrate the effectiveness of the proposed method in terms of both qualitative and quantitative measures.

Keywords: Histogram thresholding, histogram modification, ambiguity minimization, fuzzy sets, rough sets, beam theory, object extraction, edge extraction.

1. Introduction

Bi-level thresholding of the histogram of an image, due to its simplicity and ease of implementation, has been a popular technique used in various image processing tasks such as segmentation for object extraction and edge extraction from gradient information [4, 7, 23]. As the regions in an image do not

*This paper is dedicated to the memory of the father of rough sets, Prof. Zdzislaw Pawlak.

†Address for correspondence: Center for Soft Computing Research, Indian Statistical Institute, 203 B.T. Road, Kolkata, West Bengal, India 700108

have well-defined boundaries, it is natural and appropriate to use techniques those can incorporate the ambiguity in information for performing the thresholding operation. Authors in [8, 13–18, 26] have demonstrated the use of fuzzy and rough set theories to handle the ambiguity present in images while performing histogram thresholding. In [8, 13–17], minimization of the ambiguity in the information given by the gray levels of the image is carried out by optimizing various fuzziness measures such as index of fuzziness, fuzzy correlation and fuzzy geometric measures. The authors in [18] minimize the roughness in order to threshold the image by optimizing an entropy measure, which they call as the 'rough entropy of image'. In the above mentioned methods, the ambiguity is measured either from the local information (e.g. co-occurrence matrix) or from the global information (e.g. image histogram). The methods based on minimizing the ambiguity given by the global information consider only the distribution or shape of the image histogram and search for a suitable local minimum in the histogram to be assigned as the threshold value. In the absence of a unique minimum, as in the case of multi-modal histograms, the performance of such methods may depend heavily on the choice of the local minimum as the threshold value. A quite different fuzzy based approach is proposed in [26], where the authors perform the thresholding using a fuzzy measure for similarity between gray levels.

In this paper, we propose a novel bi-level histogram thresholding technique based on the beam theory of solid mechanics and information ambiguity minimization. We demonstrate its application in segmentation and edge detection for grayscale and color images. The proposed method is suitable for thresholding both unimodal and multi-modal histograms.

In the case of bi-level thresholding, where the elements of the histogram below a certain threshold belong to one of the two classes and the other elements belong to the other class, one representer for each class is always available. To give an example, for a grayscale image, the smallest and largest gray values in the image are the two representers. In our thresholding technique, the image histogram is considered as a simply supported beam [20, 25] in the shape of its distribution (histogram beam) pivoted on two sides at the element values of the representers, with a uniform force, say gravity, acting upon it. Then, the curvature due to the action of the force at each point of the histogram beam is determined using the well-known beam theory to obtain a modified histogram indicating the curvature values. This histogram modification process using the beam theory takes into account the distance of each element under consideration from the representers, along with the shape of the image histogram. Thus, the modified histogram embodies the information available from both the shape of the image histogram and the representers.

In case of a fatigue, the histogram beam will break at the point of maximum curvature (global optimum) [2, 25], which is the "weakest point" of the beam and may be considered as the suitable threshold value. Thus the use of beam theory helps in obtaining a unique choice for threshold value irrespective of whether a unique minimum is present in the image histogram. The point of maximum curvature is determined by minimizing the ambiguity in the overall information obtained after the histogram modification process. We use the theories of fuzzy and rough sets to measure the ambiguity in the information given by the modified histogram and then minimize the various measures of fuzziness and roughness to determine the threshold value. In these regards, a new measure of ambiguity called '*rough entropy of histogram*' is presented in this paper. The effectiveness of the proposed technique is shown in this paper with the help of a few illustrative experimental results.

The organization of the paper is as follows. In Section 2, the well-known beam theory is given. In Section 3, we present a few measures of ambiguity in information used in this paper including the new rough entropy measure. The proposed technique to perform bi-level thresholding of the histogram is

explained in Section 4. Qualitative and quantitative results obtained using the proposed method are presented in Section 5 and compared with those of a few popular bi-level histogram thresholding techniques. The paper concludes with Section 6 by providing an overview of the contributions made in the paper.

2. Beam Theory: Bending Moment and Curvature

A beam is a structure which is acted upon by forces perpendicular to its axis [20, 25]. Research activities related to beam theory is known to have existed from the times of Leonardo da Vinci and Galileo Galilei. Leonhard Euler and Daniel Bernoulli were the first to put together a useful theory back in the year 1750, which presented the popularly known Euler-Bernoulli beam equation [9, 20, 25]. Under the assumption

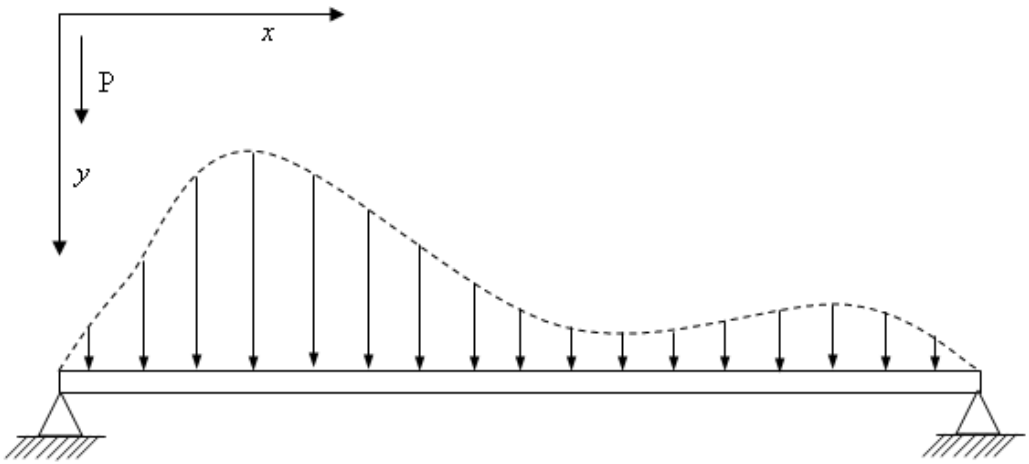

Figure 1. A simply supported beam in the shape of an image histogram

that the length of the beam is significantly larger than its width and depth, the displacement W of the beam in the direction (y) of the force is governed by the Euler-Bernoulli beam equation (see Figure 1), which is expressed as

$$E \times I \times \frac{d^4W}{dx^4} = P, \tag{1}$$

where E is the Young's modulus of the beam and I is the moment of inertia of the beam's cross-section, which are assumed to be constant in the x direction. The quantity P represents the force acting on the beam. The stress (Se) and strain (Sa) acting on the beam due to the force P are given by

$$Se = \frac{Mo \times x}{I} \quad \text{and} \tag{2}$$

$$Sa = \frac{x}{R}, \tag{3}$$

where Mo stands for the bending moment acting on the beam and R represents the radius of curvature. The curvature (ρ) of the beam is approximately expressed as

$$\rho = \frac{1}{R} = \frac{d^2W}{dx^2}. \tag{4}$$

Substituting (4) in (1), we get:

$$E \times I \times \frac{d^2\rho}{dx^2} = P \tag{5}$$

Furthermore, the magnitude of P is expressed as

$$P = \frac{d^2 Mo}{dx^2}. \tag{6}$$

From (5) and (6), we get:

$$E \times I \times \rho = Mo \tag{7}$$

The relation in (7) can also be arrived at by using the Hooke's law [20,25] which is given by the following expression:

$$E \times Se = Sa \tag{8}$$

We shall not be concerned with the value of E as it is a property of the beam material. Hence, without loss of generality, we assume $E = 1$ and arrive at a relation

$$\rho = \frac{Mo}{I}. \tag{9}$$

This relation in (9) is used in our novel histogram thresholding method (Section 4).

3. Measures of Ambiguity using Fuzzy and Rough Sets

Lofti Zadeh in the year 1965 proposed the theory of fuzzy sets, where the concept of vague boundaries of objects (sets) is used to consider the ambiguity in information [6]. Later, in the year 1982, Zdzislaw Pawlak came up with the rough set theory [19], which focuses on ambiguity as the limited discernibility of objects (sets) in the domain of discourse and is a popular mathematical framework for granular computing [18]. In this section, we explain in brief a few measures of ambiguity in images using fuzzy set theory and present a new ambiguity measure called '*rough entropy of histogram*' using rough set theory.

3.1. Ambiguity measures using fuzzy sets

Pal et al. in the year 1983 [16], pioneered the use of the concept of minimizing fuzziness measures, which quantify ambiguity in information, to perform image segmentation based on histogram thresholding. Thereafter, various articles have been written presenting the use of different measures of fuzziness in information for histogram thresholding [8, 13–15, 17, 18, 26]. A comprehensive review of fuzzy techniques of measuring uncertainty and various image segmentation techniques are given in [11] and [12], respectively.

Here, we present the few measures of ambiguity in images using fuzzy sets those we have used in this paper. It should be noted that although we explain the measures for grayscale images, they are also very well applicable to color or multi-spectral images. Consider an image X of size $M \times N$ with L gray levels. Each of the L gray levels can be mapped onto an interval $[0, 1]$, which gives the membership values denoting the degree of brightness corresponding to each gray level. Various linear and nonlinear functions are present to carry out this kind of mapping [6]. In fuzzy theory based thresholding literature,

Zadeh's S-function has been widely used to calculate the fuzzy membership values of each gray level giving its degree of brightness. The transformation using the S-function is expressed as

$$\mu_X(x_{mn}) = S(x_{mn}; a, b, c) = \begin{cases} 0 & x_{mn} \leq a \\ 2\left[\frac{(x_{mn}-a)}{(c-a)}\right]^2 & a \leq x_{mn} \leq b \\ 1 - 2\left[\frac{(x_{mn}-c)}{(c-a)}\right]^2 & b \leq x_{mn} \leq c \\ 1 & x_{mn} \geq c \end{cases}, \tag{10}$$

where x_{mn} denotes the value of gray level at the $(m,n)^{\text{th}}$ location of the image X. The cross-over point b is given by $b = (a+c)/2$ and the bandwidth is expressed as $\Delta b = b-a = c-b$. Once the membership values $\mu_X(x_{mn})$ have been calculated, they are used to determine the amount of fuzziness present in the image. Index of fuzziness is one of the popular measures which gives the average amount of ambiguity present in an image. The expression for index of fuzziness is given by:

$$\nu_p(X) = \frac{2}{(MN)^{\frac{1}{p}}} \left[\sum_m \sum_n \left[|\mu_X(x_{mn}) - \mu_{\underline{X}}(x_{mn})| \right]^p \right]^{\frac{1}{p}} \tag{11}$$
$$m = 1, 2, \ldots, M;\ n = 1, 2, \ldots, N$$

where p is an integer and $\mu_{\underline{X}}(x_{mn})$ denotes the nearest two-level version of X such that

$$\mu_{\underline{X}}(x_{mn}) = \begin{cases} 0 & \mu_X(x_{mn}) \leq 0.5 \\ 1 & \text{otherwise} \end{cases}, \tag{12}$$

When, the value of $p = 1$, the measure is called the linear index of fuzziness and when $p = 2$, it is called the quadratic index of fuzziness [16]. Fuzzy entropy [16] is an another widely used measure of ambiguity. It is given by:

$$H(X) = \frac{1}{MN} \sum_m \sum_n \left[-\mu_X(x_{mn}) \log_2(\mu_X(x_{mn})) - (1 - \mu_X(x_{mn})) \log_2(1 - \mu_X(x_{mn})) \right] \tag{13}$$
$$m = 1, 2, \ldots, M;\ n = 1, 2, \ldots, N$$

Fuzzy correlation [15], which is based on the concept of correlation between two fuzzy sets, is also an useful tool to measure ambiguity. The expression of fuzzy correlation that is used to measure the ambiguity in an image is given by:

$$C(X) = \begin{cases} 1 - \frac{4\sum_m \sum_n (\mu_X(x_{mn}) - \mu_{\underline{X}}(x_{mn}))^2}{D_1 + D_2} & D_1 + D_2 \neq 0 \\ 1 & D_1 + D_2 = 0 \end{cases} \tag{14}$$

where

$$D_1 = \sum_m \sum_n (2\mu_X(x_{mn}) - 1)^2 \quad \text{and}$$
$$D_2 = \sum_m \sum_n (2\mu_{\underline{X}}(x_{mn}) - 1)^2.$$

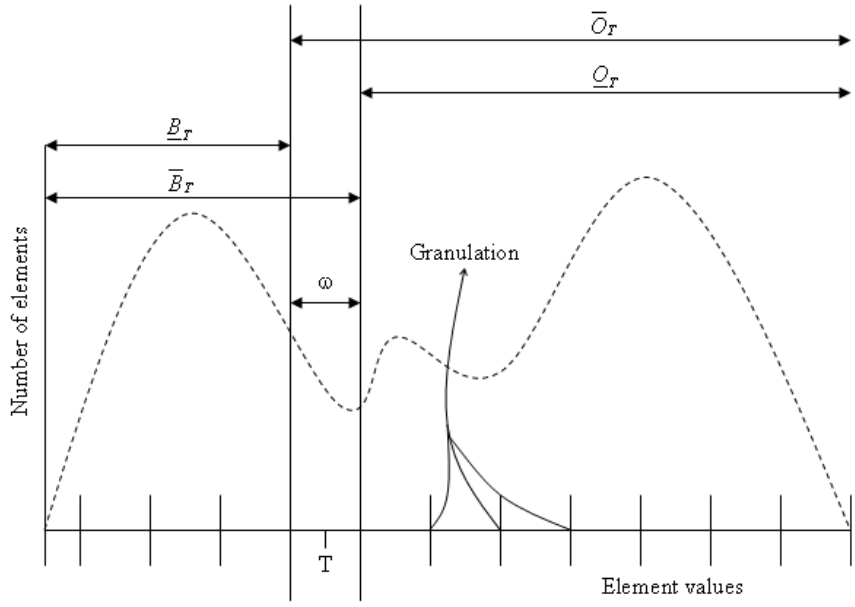

Figure 2. Granulation of an image histogram

The three measures of ambiguity given by equations (11), (13) and (14) are directly calculated from the gray values in the image and hence consider only the distribution or shape of the image histogram.

3.2. Ambiguity measures using rough sets

In 2005, Pal et al. [18] introduced the use of rough set theory in modeling ambiguity in an image and used it for image segmentation. The authors performed spatial granulation of the image to get induced equivalence classes and introduced a rough entropy measure, which was optimized to get the threshold value. Here we define a new rough entropy measure called '*rough entropy of histogram*' based on gray level granulation.

3.2.1. Rough entropy of histogram

The gray level granulation of an image histogram is shown in Figure 2. The induced equivalence classes or granules [18, 24] are obtained by partitioning the universe of the elements in an image based on their gray values. The value of T in the figure is the value of the gray level threshold under consideration and ω denotes the size of the granules. The granules are obtained such that the elements with gray value T are never boundary elements of a granule. Let the symbol O_T represent the set of elements having gray values above the threshold T, which belong to one of the two classes (say object) and B_T denote those belonging to the other class (say background). Let U be the universe of all the x_{mn} elements in the image X. The sets O_T and B_T are then expressed as:

$$O_T = \{x_{mn} \in U : \ x_{mn} > T\} \tag{15}$$

$$B_T = \{x_{mn} \in U : \ x_{mn} \leq T\} \tag{16}$$

Then using the rough set theory one can obtain the lower approximations of O_T and B_T, which are given by:

$$\underline{O}_T = \{x_{mn} \in U : [x_{mn}]_\omega \subseteq O_T\} \tag{17}$$
$$\underline{B}_T = \{x_{mn} \in U : [x_{mn}]_\omega \subseteq B_T\} \tag{18}$$

and the upper approximations of O_T and B_T are expressed as:

$$\overline{O}_T = \{x_{mn} \in U : [x_{mn}]_\omega \cap O_T \neq \emptyset\} \tag{19}$$
$$\overline{B}_T = \{x_{mn} \in U : [x_{mn}]_\omega \cap B_T \neq \emptyset\} \tag{20}$$

where $[x_{mn}]_\omega$ stands for granules of size ω. As the elements with gray value T are never boundary elements of a granule, the condition $\underline{B}_T = \overline{B}_T$ or $\underline{O}_T = \overline{O}_T$ would occur only due to the shape of the histogram.

Now the roughness of O_T and B_T are defined as:

$$R_{O_T} = 1 - \frac{|\underline{O}_T|}{|\overline{O}_T|} \tag{21}$$
$$R_{B_T} = 1 - \frac{|\underline{B}_T|}{|\overline{B}_T|} \tag{22}$$

where $|\underline{O}_T|$, $|\overline{O}_T|$, $|\underline{B}_T|$ and $|\overline{B}_T|$ are the cardinalities of the sets $\underline{O}_T$, $\overline{O}_T$, $\underline{B}_T$ and $\overline{B}_T$, respectively.

We then use these roughness measures to define the '*rough entropy of histogram*' as

$$RE_T = -\frac{1}{2}\left[R_{O_T} \log_e\left(\frac{R_{O_T}}{e}\right) + R_{B_T} \log_e\left(\frac{R_{B_T}}{e}\right)\right]. \tag{23}$$

The value of RE_T lies between 0 and 1. Note that the above measure attains the minimum value of zero only when $R_{O_T} = R_{B_T} = 0$ and the maximum value of unity only when $R_{O_T} = R_{B_T} = 1$. This concept is consistent with the fact that maximum information (entropy) is available when the uncertainty is maximum, which is the case when the roughness values are unity. Note that, this underlying concept is different from the one considered in [18]. The plot of RE_T for various values of R_{O_T} and R_{B_T} is given in Figure 3.

4. The Proposed Histogram Thresholding Technique

In literature, numerous automatic algorithms have been proposed to threshold the histogram of an image. Most of these algorithms are based on the shape of the histogram and are designed to find an appropriate valley in the histogram [7]. Such algorithms would perform very well when the histogram is predominantly bimodal. However, in case of unimodal or multi-modal (no. of modes > 2) histograms, these algorithms might give unsatisfactory results. The authors in [22] and [29] attempted to deal with such problems by carrying out histogram modification or by finding the 'shoulder' in the histogram instead of the valley. A few approaches to threshold a histogram were proposed in [10, 21, 27], whose performance do not depend on the modal characteristics of the histogram. However, these classical approaches do not

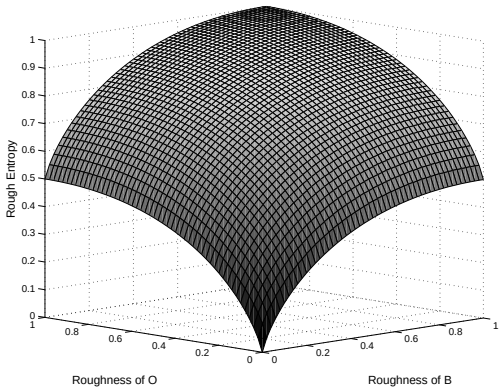

(a) Plot of rough entropy for various roughness values (R_{O_T} and R_{B_T})

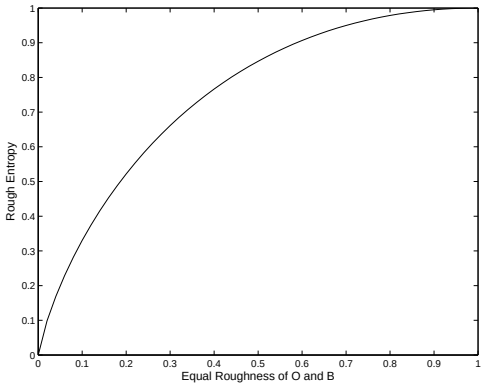

(b) Plot of rough entropy for roughness values $R_{O_T} = R_{B_T}$ (i.e. when $|\underline{O}_T| = |\underline{B}_T|$ [18])

Figure 3. Plots of the proposed rough entropy of histogram

consider the ambiguity present in the information and hence the two regions obtained after the bi-level thresholding process might not be acceptable.

In this section, we present a novel method for bi-level thresholding of image histogram using beam theory and ambiguity measures. Beam theory is used to carryout a histogram modification process that considers the distance of each element from the representers of the two classes along with the shape of the histogram. As the modified histogram not only contains the information available from the shape of the image histogram but also that from the representers, it could be useful in determining a unique threshold value in cases where various ambiguity minimization processes applied to image histograms produce inconclusive results.

4.1. The proposed methodology

As shown in Figure 4, first the image histogram is subjected to the beam theory based histogram modification process. Then, the ambiguity minimization in the overall information given by the modified histogram is carried out.

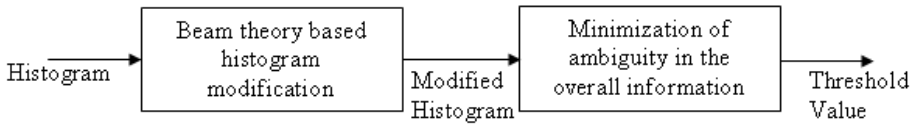

Figure 4. Block diagram of the proposed technique

For the histogram modification process, we consider the histogram as a simply supported beam in the shape of its distribution pivoted on two sides at the element values of the representers and call it the histogram beam. According to [20], "A member of a structure which is acted upon by forces perpendicular to its axis is called a beam. A beam which rests freely on two supports is called a simply

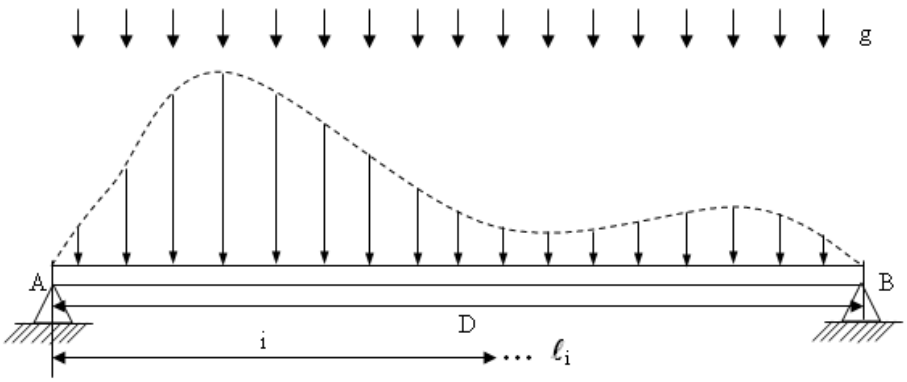

Figure 5. Load on a Histogram Beam

supported beam". We consider that a uniform force, say gravity (g), acts upon the histogram beam. Therefore, the overall force per unit length on the histogram beam, which corresponds to the force acting upon each bin of the histogram, will have a linear relationship with the height of the bins. The bending moment (Mo_{l_i}) at each bin (l_i) of the histogram (refer Figure 5) due to the force (load) is calculated as:

$$Mo_{l_i} = (R_A \times i) - (CP_{l_i} \times [i - COG_{l_i}]) \quad (24)$$
$$i = 0, 1, \ldots, D \text{ and } l_i = i + 1$$

where D is the length of the histogram beam and R_A is the reactive force at the pivot A due to the total load on the histogram beam. The value of i is the distance of the bin l_i from the pivot A. The total load between the points A and l_i is given by CP_{l_i}. The symbol COG_{l_i} stands for the center of gravity of the beam between the points A and l_i. The reactive force R_A is calculated as

$$R_A = CP_{l_{D+1}} \times \left[\frac{D - COG_{l_{D+1}}}{D}\right]. \quad (25)$$

The center of gravity COG_{l_i} is calculated using the expression

$$COG_{l_i} = \frac{1}{\sum_{k=1}^{l_i} P_k} \sum_{k=1}^{l_i} (k-1)P_k, \quad (26)$$

where P_k is the load at the k^{th} bin. As mentioned earlier, this load has a linear relationship with the histogram value at that bin. Hence, without loss of generality, we consider $P_k = H_k + \Upsilon$, where H_k is the height of the k^{th} bin of the histogram and Υ is any finite constant value with $\Upsilon > 0$.

Next, using (9), we calculate the curvature value at each bin due to the action of the bending moment given by (24) as follows

$$CUR_{l_i} = \frac{Mo_{l_i}}{I_{l_i}}, \quad (27)$$

where I_{l_i} is value of the moment of inertia at l_i. This value of I_{l_i} is calculated using

$$I_{l_i} = \frac{1}{\sum_{k=1}^{l_i} P_k} \sum_{p=1}^{l_i} \sum_{q=0}^{P_p} (q - m_p)^2. \quad (28)$$

The symbol m_p denotes the centroid of the load P_p acting at the p^{th} bin. Note that the centroid of the load corresponds to the centroid of the histogram beam at p. Once the value of CUR_{l_i} has been obtained, we perform the following transformation:

$$ACUR_{l_i} = \max(\mathbf{CUR}) - CUR_{l_i} \tag{29}$$

where $\mathbf{CUR} = \{CUR_{l_i}\},\ l_i = 1, 2, \ldots, D+1$. The $ACUR_{l_i}$ are the values of the modified histogram.

The above process of histogram modification (equations (24)-(29)) considers the information from both the shape of the histogram and the representers. It is well known that in case of a fatigue, the histogram beam will break at the point of maximum curvature [2, 25], which is the "weakest point" in the beam. Hence, it is quite natural to consider the point of maximum curvature along the length of the histogram beam as the threshold value. Interestingly, this consideration is analogous to the minimization of the ambiguity in the information given by the values ($ACUR_{l_i}$) of the modified histogram. Hence, various ambiguity minimization based histogram thresholding algorithms can be applied to the modified histogram in order to obtain a suitable threshold value that would correspond to the point (element value) of maximum curvature.

In this paper, we use the theory of fuzzy sets and rough sets to perform the ambiguity minimization process. In case of fuzzy set theory based ambiguity minimization, we calculate the fuzzy membership value of each element corresponding to the modified histogram using the Zadeh's S-function given in (10). As explained in Section 3, the membership values are then used to calculate the fuzziness in the information using the linear index of fuzziness, fuzzy entropy and fuzzy correlation measures given in (11), (13)and (14), respectively. The fuzziness is measured across the modified histogram by varying the cross-over point of the S-function such that it takes all the element values. Then, the element value for which the fuzziness is minimum is considered as the threshold value. Thus, fuzzy-optimal thresholds based on ambiguity minimization using the above mentioned fuzziness measures are obtained.

Rough set theory based ambiguity minimization is carried out by employing the technique described in Section 3. The upper and lower approximations of the two ambiguous classes regarding bi-level thresholding of the modified histogram are determined using equations (17)-(20). The roughness in the information corresponding to the two classes is calculated using (21) and (22). Then, the rough entropy of the information given by the modified histogram is measured using (23). This entropy measure is determined across the modified histogram by varying the value of T in (15) and (16) such that it takes all the element values. Then, the element value for which the value of rough entropy is minimum is considered as the rough-optimal threshold value.

Thus, a suitable threshold value is determined for a given histogram by first carrying out a beam theory based modification that considers a distance measure apart from the shape of the histogram and then by performing ambiguity minimization.

4.2. Consequences of the beam theory based histogram modification

Using a few typical cases, we shall now present the effect of the having a beam theory based histogram modification process, which helps in obtaining a unique threshold value, before the ambiguity minimization is carried out to determine the threshold value.

Figure 6 shows a few typical non-bimodal histogram where the ambiguity minimization processes produce unclear results and the inclusion of the beam theory based histogram modification helps to overcome such problems. The histogram shown in Figure 6(a)&(b) has a trimodal distribution. The ambig-

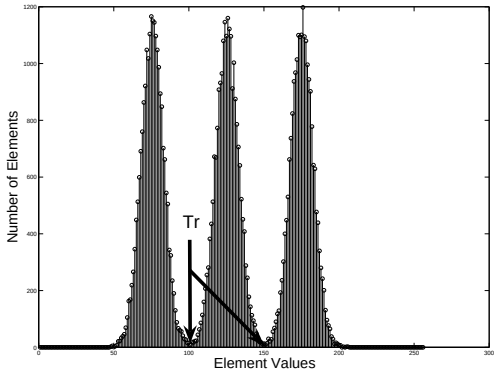

(a) Ambiguity minimization

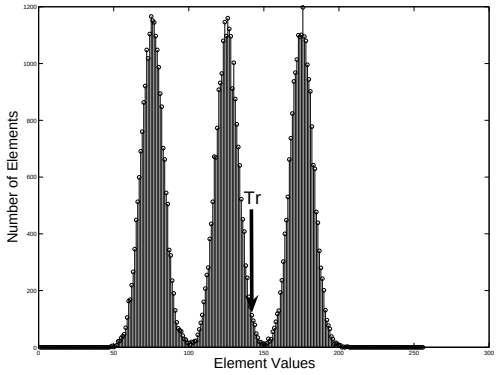

(b) Histogram modification + ambiguity minimization

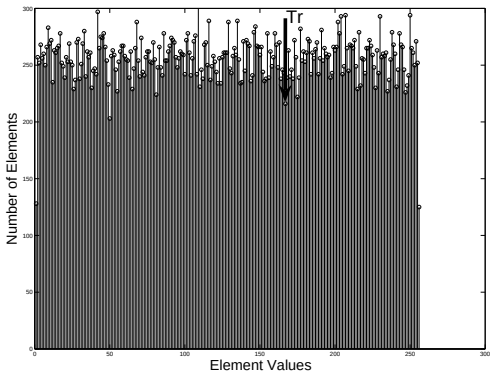

(c) Ambiguity minimization

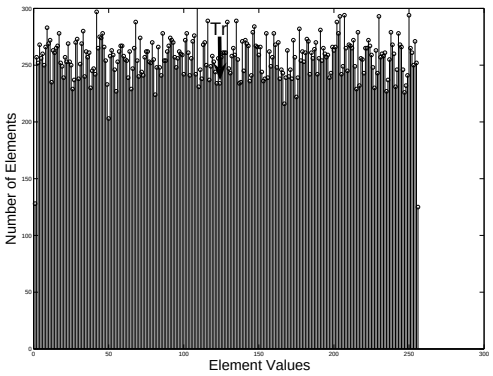

(d) Histogram modification + ambiguity minimization

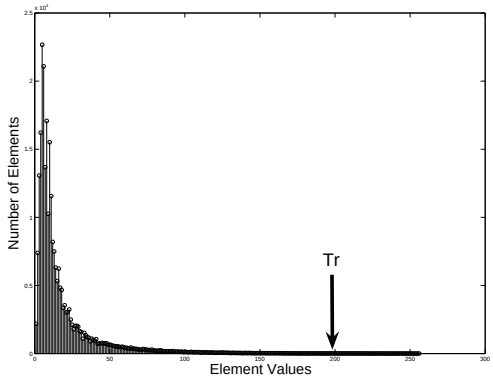

(e) Ambiguity minimization

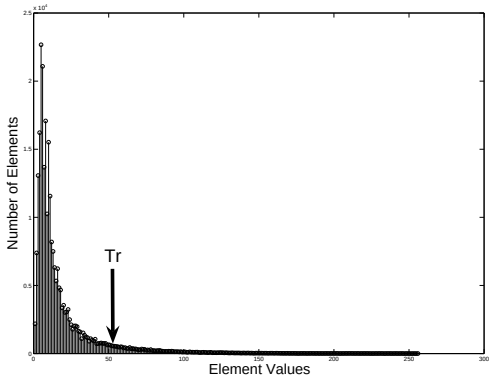

(f) Histogram modification + ambiguity minimization

Figure 6. Threshold determination in a few typical non-bimodal histograms (Tr → Threshold value)

uity minimization process results in two equally good thresholds, whereas the inclusion of the histogram modification process overcomes this problem. The histogram in Figure 6(c)&(d) is of an image with five different gray level regions having uniformly-distributed texture. Although the ambiguity minimization process gives a particular threshold, many other threshold values were found to have minimized the ambiguity to a similar level. On the other hand, as expected for an uniform distribution, the threshold value determined with the histogram modification process is near the middle of the dynamic range. Figure 6(e)&(f) displays an unimodal distribution, where the introduction of the histogram modification process helps to arrive at an acceptable threshold value.

As shown in Figure 7, in case of bimodal histograms, the histogram modification process does not make much of a difference to the selected threshold value when compared with the threshold value obtained by carrying out the ambiguity minimization process alone.

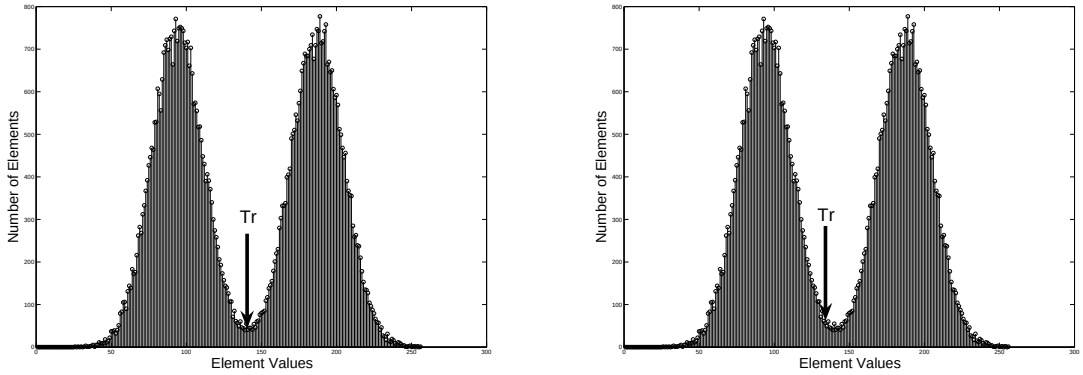

(a) Ambiguity minimization (b) Histogram modification + ambiguity minimization

Figure 7. Threshold determination in a typical bimodal histogram (Tr → Threshold value)

5. Experimental Results and Comparisons

In this section, the performance of the proposed bi-level histogram thresholding technique is compared with those of a few existing ambiguity minimization based thresholding algorithms and a few popular classical techniques. The methods are applied to carry out object extraction using global histogram and edge extraction using gradient histogram. The gradient values are obtained by applying the Canny operator [3, 5] to the gray level or color images. The techniques considered for comparison with that of the proposed one are (i) thresholding using index (linear) of fuzziness [16], (ii) thresholding using fuzzy entropy [16], (iii) thresholding based on fuzzy correlation [15], (iv) rough entropy based thresholding (refer Section 3), (v) fuzzy gray level similarity based thresholding [26], (vi) Otsu's method [10], (vii) Pun's method [21], (viii) Tsai's method [27]. The proposed technique is implemented using four different measures of ambiguity and may be referred to as (ix) beam theory & index of fuzziness, (x) beam theory & fuzzy entropy, (xi) beam theory & fuzzy correlation, and (xii) beam theory & rough entropy based methods. These methods will henceforth be referred using their corresponding numbers in the paper. Both quantitative and qualitative results are presented. We shall refer to the proposed algorithms (ix)-(xii) as a single proposed method because these four algorithms are based on a single concept of beam

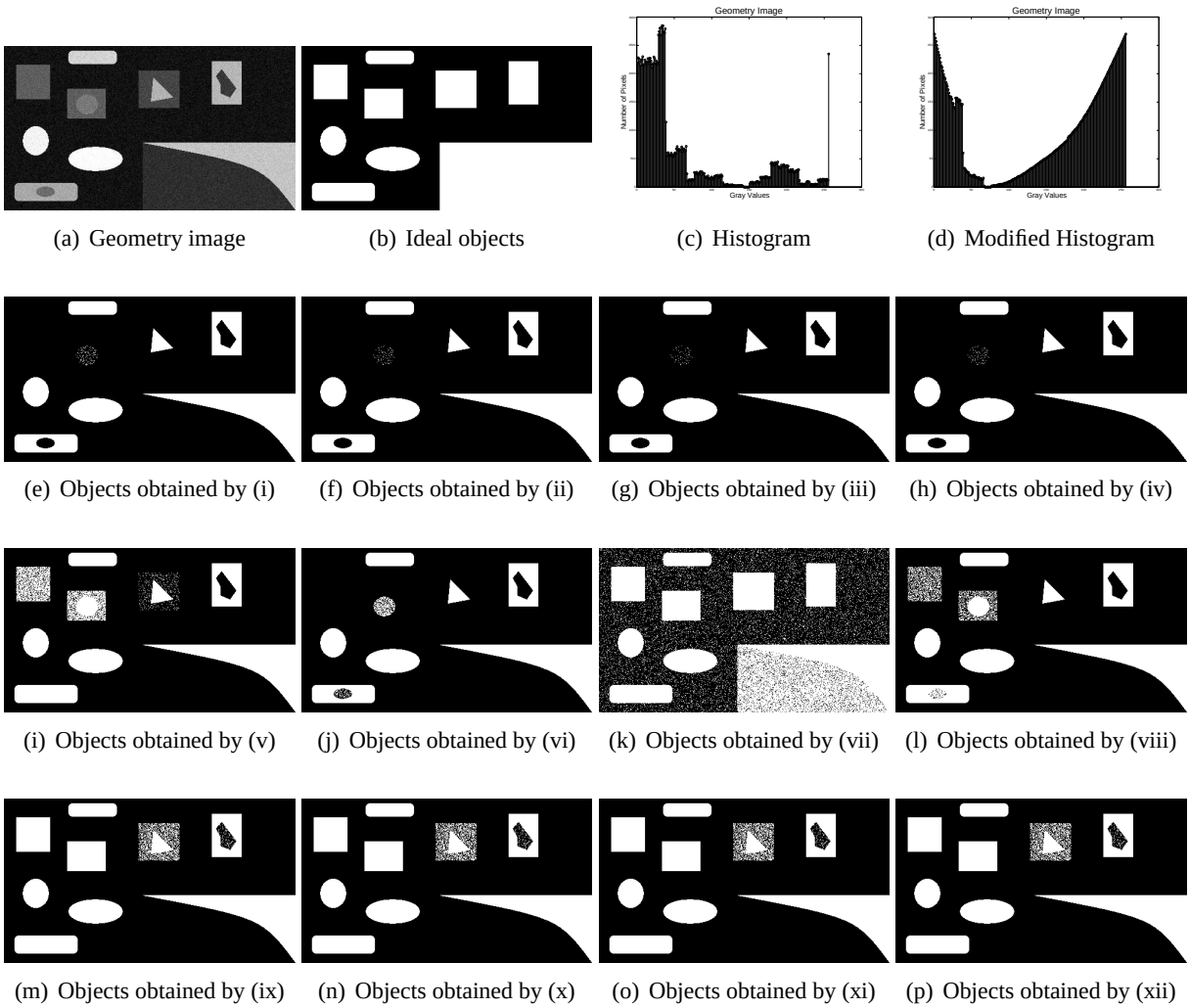

(a) Geometry image (b) Ideal objects (c) Histogram (d) Modified Histogram

(e) Objects obtained by (i) (f) Objects obtained by (ii) (g) Objects obtained by (iii) (h) Objects obtained by (iv)

(i) Objects obtained by (v) (j) Objects obtained by (vi) (k) Objects obtained by (vii) (l) Objects obtained by (viii)

(m) Objects obtained by (ix) (n) Objects obtained by (x) (o) Objects obtained by (xi) (p) Objects obtained by (xii)

Figure 8. Qualitative results obtained using various thresholding techniques to perform object extraction on the synthetically generated 'Geometry' image

theory based histogram modification followed by ambiguity minimization. As suggested in [14], during the ambiguity minimization process, the bandwidth of S-function (Δb) and the size of granules (ω) are varied over a range in order to choose the most consistent threshold value. It is to be noted that in the proposed method, it is assumed that no prior information about the classes is available and hence the smallest and the largest element values in the histogram are considered as the representers. The quantitative results are presented for a synthetically generated image which we refer to as the 'Geometry' image. A remote sensing image called the 'Montreal' image, a medical image called the 'Angiography' image and two color images called the 'Fluorescent cells' image & 'Nisyros island' image are also used in this section.

Figures 8 and 9 give the qualitative results of the various techniques in extracting the objects from the background and edges from the gradient values when applied on the synthetically generated 'Geometry'

image. Figures 8(b) and 9(b) show the ideal object and edge extraction results, respectively. Figures 8(c)&(d) and 9(c)&(d) give the histogram and modified histogram under consideration for object and edge extraction, respectively.

From Figure 8, it is evident that the proposed technique performs better object extraction compared to the others. The result obtained using (v) is nearest to the proposed one. But, it's performance is dependent on a required prior information in the form of seed points. The knowledge of suitable seed points is essential for the implementation of the algorithm [26].

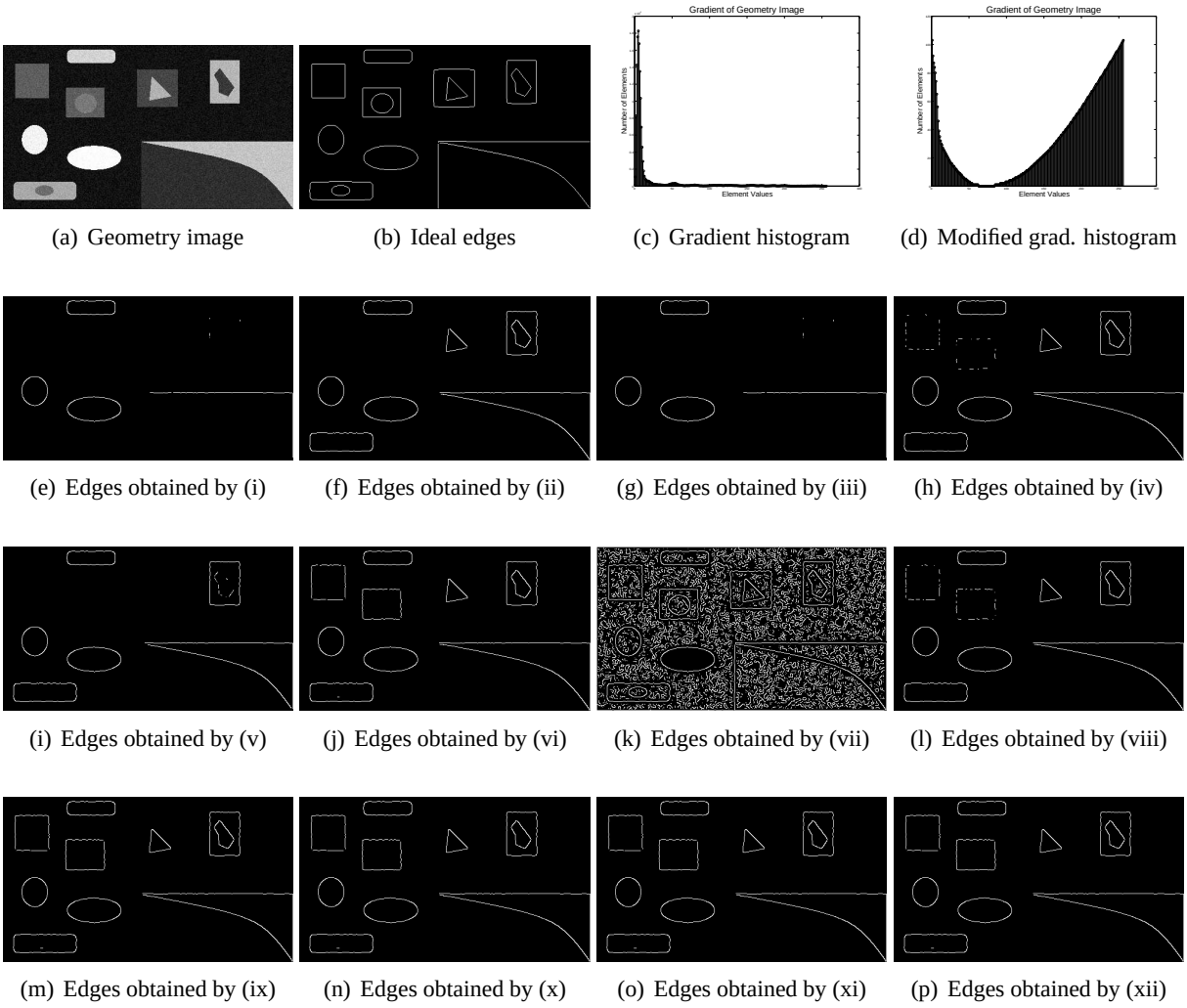

(a) Geometry image (b) Ideal edges (c) Gradient histogram (d) Modified grad. histogram

(e) Edges obtained by (i) (f) Edges obtained by (ii) (g) Edges obtained by (iii) (h) Edges obtained by (iv)

(i) Edges obtained by (v) (j) Edges obtained by (vi) (k) Edges obtained by (vii) (l) Edges obtained by (viii)

(m) Edges obtained by (ix) (n) Edges obtained by (x) (o) Edges obtained by (xi) (p) Edges obtained by (xii)

Figure 9. Qualitative results obtained using various thresholding techniques to perform edge extraction on the gradient of synthetically generated 'Geometry' image

Our technique does not require any such prior information. However, if the seed points are available, they can be used as the representers (pivots) instead of the smallest and the largest element values. One can depict from Figure 9 that the proposed technique outperforms all the others in determining a threshold value from the gradient histogram to extract the edges. The thinning of the edges is done by applying the non-maximal suppression algorithm [3] after applying the threshold determined from the gradient histogram.

Techniques:→	(i)	(ii)	(iii)	(iv)	(v)	(vi)
Object extraction (MSE)	15217	15242	15250	15242	12437	14920
Object extraction (MSSIM)	0.711	0.711	0.711	0.711	0.742	0.712
Edge extraction (FOM)	0.197	0.477	0.197	0.506	0.516	0.569

Techniques:→	(vii)	(viii)	(ix)	(x)	(xi)	(xii)
Object extraction (MSE)	5865.5	13373	11003	11003	11003	11003
Object extraction (MSSIM)	0.278	0.728	0.792	0.792	0.792	0.792
Edge extraction (FOM)	0.159	0.526	0.572	0.572	0.572	0.572

Table 1. Quantitative results obtained using various bi-level thresholding techniques on the synthetically generated 'Geometry' image

Table 1 gives the quantitative results of the various thresholding techniques. The mean square error (MSE) and the mean structural similarity measures (MSSIM) [28] between the ideal and the actual object extraction results are given. The MSE gives the the amount of non-similarity between pixels of the two images at identical locations, whereas the MSSIM gives the similarity in the structures present in both the images. The MSSIM measure may be considered as the more meaningful measure of similarity as it is closer to the human visual perception [28]. A lower value of MSE and a higher value of MSSIM indicates better performance. A figure of merit (FOM) measure defined by Abdou et al. [1] to evaluate edge extraction performance is used in this paper. The FOM measures the similarity in the location of the edges in the two images and hence can be readily used to evaluate the edge extraction performance of the thresholding methods. A higher value of FOM indicates better performance. It is evident from the table that the proposed thresholding technique gives consistently good quantitative results for different kinds of histograms such as gray level multi-modal histogram and gradient unimodal histogram.

Figures 10 and 11 show the qualitative results of the various thresholding techniques using the 'Montreal' image, which is a remote sensing image.

This image, which shows the land and river regions in the city of Montreal, has been obtained from the website of Natural Resources Canada. It is seen from Figure 10 that all the methods except (v) and the proposed one put the river and land in the same segment. In the segmentation carried out by (v), a larger part of the land is assigned to the region of the river compared to that of the proposed method and hence the proposed technique may be considered as better than the others. As seen in Figure 11, methods (i)-(v) eliminate a lot of correct edges along with the false edges. On the other hand, methods

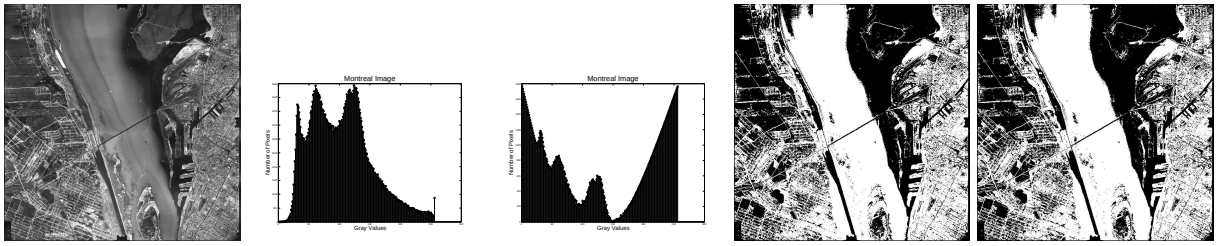

(a) Montreal image (b) Histogram (c) Modified histogram (d) Objects by (i) (e) Objects by (ii)

(f) Objects by (iii) (g) Objects by (iv) (h) Objects by (v) (i) Objects by (vi) (j) Objects by (vii)

(k) Objects by (viii) (l) Objects by (ix) (m) Objects by (x) (n) Objects by (xi) (o) Objects by (xii)

Figure 10. Qualitative results obtained using various thresholding techniques to perform object extraction on the 'Montreal' remote sensing image

(vi)-(viii) leave behind significant amount of false edges. Compared to these methods the proposed one gives visibly better results loosing a very few correct edges and retaining a few false edges.

Figures 12 and 13 show the qualitative results of the various thresholding techniques using the 'Angiography' image, which is a medical image. It is evident from the results given in Figure 12 that only the proposed method is able to extract out all the blood vessels from the background.

On the other hand, all the other techniques except method (vii) fail in extracting out the thinner blood vessels. When the proposed method is applied to threshold the gradient histogram of the 'Angiography' image, it succeeds in accurately extracting the edges. However, methods (vi) and (viii) also perform equally well. Hence, in this case, the proposed method is equally good or better than the other techniques.

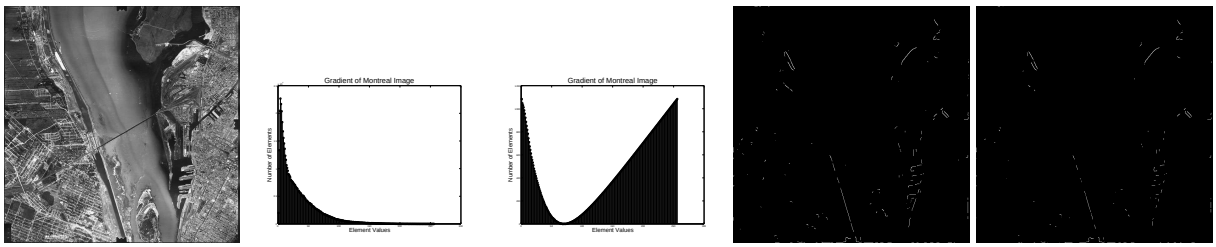

(a) Montreal image (b) Gradient histogram (c) Modified grad. hist. (d) Edges by (i) (e) Edges by (ii)

(f) Edges by (iii) (g) Edges by (iv) (h) Edges by (v) (i) Edges by (vi) (j) Edges by (vii)

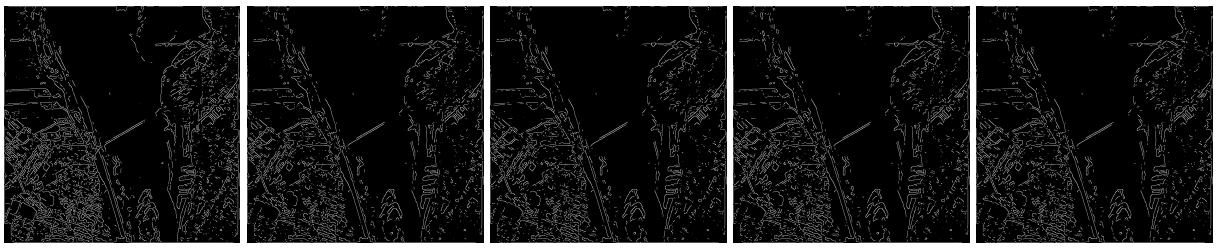

(k) Edges by (viii) (l) Edges by (ix) (m) Edges by (x) (n) Edges by (xi) (o) Edges by (xii)

Figure 11. Qualitative results obtained using various thresholding techniques to perform edge extraction on the gradient of 'Montreal' remote sensing image

Table 2 enlists the threshold values obtained by using the various algorithms for object extraction (obj.) and edge extraction (edg.) purposes in the 'Geometry', 'Montreal' and 'Angiography' Images. Note that the values given in the form of an array for the method (v) are the seed element values, which are essential for the implementation of the method. We normalize the element values of all kinds of images to the dynamic range [0, 255].

Figure 14 presents the use of the proposed methodology of beam theory based modification followed by rough-optimal threshold determination (method (xii)) in color images. The two color images considered are the 'Fluorescent cells' image obtained from the website of University of Camerino, Italy and the 'Nisyros island' image, a remote sensing image obtained from the website of National Aeronautics and Space Administration, USA.

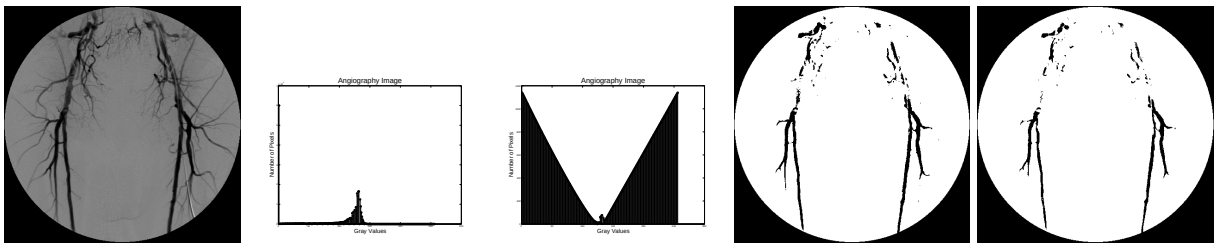

(a) Angiography image (b) Histogram (c) Modified histogram (d) Objects by (i) (e) Objects by (ii)

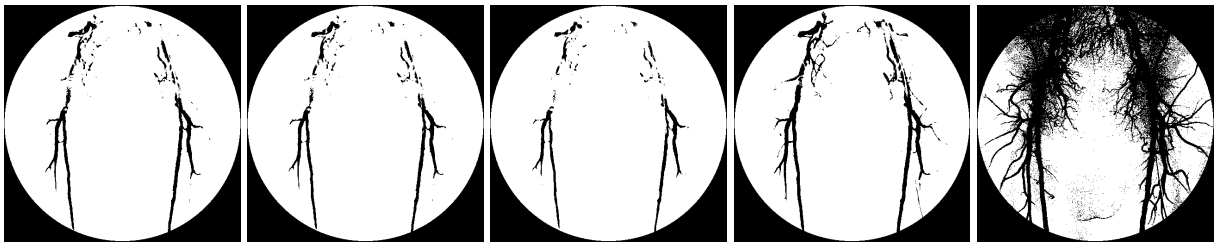

(f) Objects by (iii) (g) Objects by (iv) (h) Objects by (v) (i) Objects by (vi) (j) Objects by (vii)

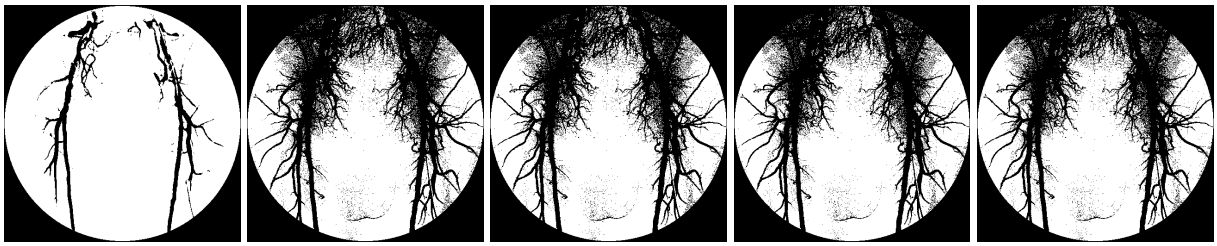

(k) Objects by (viii) (l) Objects by (ix) (m) Objects by (x) (n) Objects by (xi) (o) Objects by (xii)

Figure 12. Qualitative results obtained using various thresholding techniques to perform object extraction on the 'Angiography' medical image

Figure 14(b)&(e) are the results of thresholding each component of the color images using the method (xii), adding the three thresholded images to produce an image having more than two segmented regions and then using the average of the three threshold values on the added image to obtain the final two segments. Note that typical ways of handling the three color components while performing object extraction in a color image is given in [4]. Figures 14(c)&(f) are the results obtained by thresholding the color gradient of the images calculated using the color Canny operator [5]. Here, the non-maximal suppression algorithm has not been applied unlike the previously shown qualitative edge extraction results.

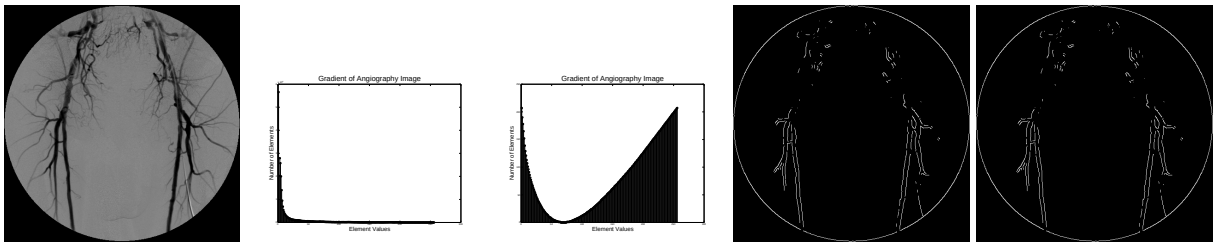

(a) Angiography image (b) Gradient histogram (c) Modified grad. hist. (d) Edges by (i) (e) Edges by (ii)

(f) Edges by (iii) (g) Edges by (iv) (h) Edges by (v) (i) Edges by (vi) (j) Edges by (vii)

(k) Edges by (viii) (l) Edges by (ix) (m) Edges by (x) (n) Edges by (xi) (o) Edges by (xii)

Figure 13. Qualitative results obtained using various thresholding techniques to perform edge extraction on the gradient of 'Angiography' medical image

Techniques:→	(i)		(ii)		(iii)		(iv)	
Images	obj.	edg.	obj.	edg.	obj.	edg.	obj.	edg.
Geometry	135	175	137	90	138	175	137	81
Montreal	89	151	89	163	89	151	89	147
Angiography	40	98	31	97	44	99	40	93

Techniques:→	(v)		(vi)		(vii)		(viii)	
Images	obj.	edg.	obj.	edg.	obj.	edg.	obj.	edg.
Geometry	85 [50 246]	131 [25 231]	115	73	33	5	95	79
Montreal	174 [45 246]	140 [100 236]	104	46	100	26	117	54
Angiography	33 [10 110]	128 [50 236]	64	50	123	5	75	58

Techniques:→	(ix)		(x)		(xi)		(xii)	
Images	obj.	edg.	obj.	edg.	obj.	edg.	obj.	edg.
Geometry	70	71	70	71	70	71	70	71
Montreal	147	67	147	68	147	67	148	69
Angiography	122	67	123	67	122	67	123	67

Table 2. Threshold values obtained using various techniques for object and edge extraction purposes

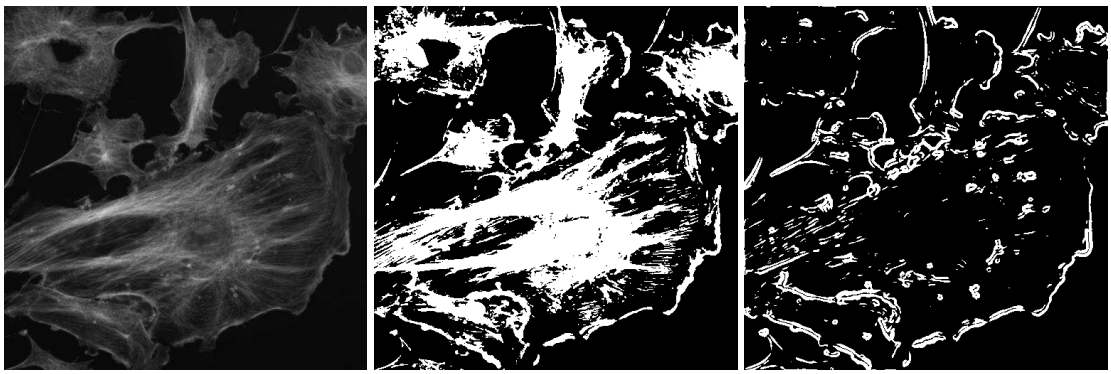

(a) Fluorescent cells (intensity image) (b) Color value Thresholding (c) Gradient value Thresholding

(d) Nisyros island (intensity image) (e) Color value Thresholding (f) Gradient value Thresholding

Figure 14. Segmentation of color images and their gradients using the proposed beam theory based histogram modification and rough entropy based optimization

6. Conclusion

The issue of bi-level thresholding in images taking into account their inherent ambiguity has been considered in this paper. It has been found that the existing ambiguity minimization based global thresholding techniques do not give satisfactory results consistently when used on various images with different histograms. In this paper, an analogy has been drawn between the concept of the beam theory in solid mechanics and the global histogram thresholding process. The histogram has been considered as a simply supported beam and then the beam theory has been used to perform a histogram modification process by calculating the curvature values corresponding to each element of the histogram. Then, various ambiguity minimization based techniques have been applied to the modified histogram in order to determine the threshold value. It has been found that such an histogram modification process considers a distance measure along with the shape of the histogram and thus helps the ambiguity minimization processes to give consistently acceptable results. With regards to the ambiguity minimization process, a new rough entropy measure of histogram has been given, which is based on the rough set theory.

Qualitative and quantitative performance of the proposed method have been studied and compared to those of a few existing ambiguity minimization based thresholding techniques and a few classical techniques. Images those have different histogram shapes and are used for different applications have been considered in this paper in order to show the results. It has been found that the proposed technique consistently performs as good as or better than the others.

References

[1] Abdou, I. E., Pratt, W. K.: Quantitative design and evaluation of enhancement/thresholding edge detectors, *Proc. IEEE*, **67**(5), 1979, 753–763.

[2] Audoly, B., Neukirch, S.: Fragmentation of rods by cascading cracks: why spaghetti do not break in half, *Physical Review Letters*, **95**, 2005, 095505 1–4.

[3] Canny, J.: A computational approach to edge detection, *IEEE Trans. Pattern Anal. Machine Intell.*, **8**(6), 1986, 679–698.

[4] Cheng, H. D., Jiang, X. H., Sun, Y., Wang, J.: Color image segmentation: advances and prospects, *Pattern Recognition*, **34**(12), 2001, 2259–2281.

[5] Kanade, T.: Image understanding research at CMU, *Proceedings of Image Understanding Workshop*, II, 1987.

[6] Klir, G., Yuan, B.: *Fuzzy sets and fuzzy logic: theory and applications*, Prentice Hall, New Delhi, India, 2005.

[7] Lee, S. U., Chung, S. Y., Park, R. H.: A comparative performance study of several global thresholding techniques for segmentation, *Computer Vision, Graphics and Image Processing*, **52**(2), 1990, 171–190.

[8] Murthy, C. A., Pal, S. K.: Histogram thresholding by minimizing graylevel fuzziness, *Information Sciences*, **60**(1-2), 1992, 107–135.

[9] Nayfeh, A. H., Pai, P. F.: *Linear and nonlinear structural mechanics*, Wiley Series in Nonlinear Science, John Wiley & Sons, New York, USA, 2004.

[10] Otsu, N.: A threshold selection method from gray-level histogram, *IEEE Trans. Syst., Man, Cybern.*, **9**(1), 1979, 62–66.

[11] Pal, N. R., Bezdek, J. C.: Measuring Fuzzy Uncertainity, *IEEE Trans. Fuzzy Syst.*, **2**(2), 1994, 107–118.

[12] Pal, N. R., Pal, S. K.: A review on image segmentation techniques, *Pattern Recognition*, **26**(9), 1993, 1277–1294.

[13] Pal, S. K., Ghosh, A.: Index of area coverage of fuzzy image subsets and object extraction, *Pattern Recognition Letters*, **11**(12), 1990, 831–841.

[14] Pal, S. K., Ghosh, A.: Fuzzy geometry in image analysis, *Fuzzy Sets and Systems*, **48**(1), 1992, 23–40.

[15] Pal, S. K., Ghosh, A.: Image segmentation using fuzzy correlation, *Information Sciences*, **62**(3), 1992, 223–250.

[16] Pal, S. K., King, R. A., Hashim, A. A.: Automatic grey level thresholding through index of fuzziness and entropy, *Pattern Recognition Letters*, **1**(3), 1983, 141–146.

[17] Pal, S. K., Rosenfeld, A.: Image enhancement and thresholding by optimization of fuzzy compactness, *Pattern Recognition Letters*, **7**(2), 1988, 77–86.

[18] Pal, S. K., Shankar, B. U., Mitra, P.: Granular computing, rough entropy and object extraction, *Pattern Recognition Letters*, **26**(16), 2005, 2509–2517.

[19] Pawlak, Z.: *Rough sets: theoritical aspects of reasoning about data*, Kluwer Academic, Dordrecht, Netherlands, 1991.

[20] Prasad, I. B.: *Applied mechanics and strength of materials*, 5th edition, Khanna Publishers, Delhi, India, 1983.

[21] Pun, T.: Entropic thresholding: a new approach, *Computer Graphics and Image Processing*, **16**, 1981, 210–239.

[22] Rosenfeld, A., Torre, P. D. L.: Histogram concavity analysis as an aid in threshold selection, *IEEE Trans. Syst., Man, Cybern.*, **13**(3), 1983, 231–235.

[23] Sezgin, M., Sankur, B.: Survey over image thresholding techniques and quatitative performance evaluation, *Journal of Electronic Imaging*, **13**(1), 2004, 146–168.

[24] Skowron, A., Rauszer, C.: The discernibility matrices and functions in information systems, *Slowiński, R., (Ed.), Intelligent Decision Support, Handbook of Applications and Advances of the Rough Sets Theory*, 1992.

[25] Timoshenko, S.: *Strength of materials*, 3rd edition, Nostrand, London, England, 1958.

[26] Tobias, O. J., Seara, R.: Image segmentation by histogram thresholding using fuzzy sets, *IEEE Trans. Image Processing*, **11**(12), 2002, 1457–1465.

[27] Tsai, W.-H.: Moment-preserving thresholding: a new approach, *Computer Vision, Graphics, and Image Processing*, **29**, 1985, 377–393.

[28] Wang, Z., Bovik, A. C., Sheikh, H. R., Simoncelli, E. P.: Image quality assesment: from error visibility to structural similarity, *IEEE Trans. Image Processing*, **13**(4), 2004, 600–612.

[29] Wezka, J. S., Rosenfeld, A.: Histogram modification for threshold selection, *IEEE Trans. Syst., Man, Cybern.*, **9**(1), 1979, 38–52.